



# The effect of nanoparticles on gastrointestinal release from modified $\kappa$ -carrageenan nanocomposite hydrogels

Hadi Hezaveh, Ida Idayu Muhamad \*

Faculty of Chemical Engineering, Universiti Teknologi Malaysia, Johor Bahru, 81310 Johor, Malaysia

## ARTICLE INFO

### Article history:

Received 30 January 2012

Received in revised form 20 February 2012

Accepted 22 February 2012

Available online 1 March 2012

### Keywords:

Nanocomposite hydrogels

Modified  $\kappa$ -carrageenan

Nanoparticles

Controlled drug release

## ABSTRACT

In this article, silver and magnetite nanofillers were synthesized in modified  $\kappa$ -carrageenan hydrogels using the in situ method. The effect of metallic nanoparticles in gastro-intestinal tract (GIT) release of a model drug (methylene blue) has been investigated. The effect of nanoparticles loading and genipin cross-linking on GIT release of nanocomposite is also studied to finally provide the most suitable drug carrier system. In vitro release studies revealed that using metallic nanocomposites hydrogels in GIT studies can improve the drug release in intestine and minimize it in the stomach. It was found that cross-linking and nanofiller loading can significantly improve the targeted release. Therefore, applying metallic nanoparticles seems to be a promising strategy to develop GIT controlled drug delivery.

© 2012 Elsevier Ltd. All rights reserved.

## 1. Introduction

In recent decades, an increasing interest has been devoted to the development of bio polymeric networks such as hydrogels due to their unique physical and chemical characteristics which makes them sensitive and intelligent materials. The existence of hydrophilic groups such as  $-\text{OH}$ ,  $-\text{COOH}$ ,  $-\text{NH}_2$ ,  $-\text{CONH}_2$ ,  $-\text{SO}_3\text{H}$  (Chern, Lee, & Hsieh, 2004) in hydrogels backbone has enabled them to imbibe large quantities of water as well as to encapsulate bio active materials within their network. These advantages have made hydrogels a suitable carrier for pharmaceutical applications such as oral drug delivery of insulin and cyclosporine (Tan, Choong, & Dass, 2010), wound dressing, tissue engineering, and so on (Chen, Liu, & Chen, 2009; Mi, Tan, Liang, & Sung, 2002; Tan et al., 2010). Application of biodegradable hydrogels has been growing due to their degradation into physiologically occurring compounds that can be readily excreted from the body (Kakinoki, Taguchi, Saito, Tanaka, & Tateishi, 2007) therefore there is no need to remove these polymers from the body at the end of the treatment period.

Metal nanoparticles (NPs) with a high specific surface area and a high fraction of surface atoms, have been studied extensively because of their unique physicochemical characteristics including catalytic activity, electronic properties, antimicrobial activity, magnetic properties and biomedical applications (Hezaveh, Fazlali, & Noshadi, 2012; Nagireddy et al., 2011; Souza et al., 2004). Among different nanoparticles, silver nanoparticles (Ag-NPs) and

magnetic nanoparticles (MNPs) have been known to have bactericidal effects, medical drug delivery applications, MRI contrast agents and so on (Cho, Park, Osaka, & Park, 2005; Laurent et al., 2008). It is expected that the combination of NPs and pH sensitive hydrogels constitute a novel functional composite keeping both hydrogel and NPs properties (Xiang & Chen, 2007).

One obstacle in preparation of nanocomposites is agglomeration of NPs due to strong magnetic dipole–dipole attractions between particles. To overcome this, different surfactants such as oleic acid, silane, or organosilane have been employed. These NPs are dispersed in monomer and polymerize the reaction mixture using initiators (Cai et al., 2007; Chen, Liu, Lin, & Yen, 2008; Hezaveh et al., 2012; Reddy, Lee, Gopalan, & Kang, 2007). To reduce the number of processing steps and time, in situ method is the most suitable approach to prepare polymeric nanocomposites, since it reduces number of synthesis steps, saves time and does not need the addition of dispersants in the solution. Saravanan, Padmanabha Raju, and Alam (2007) successfully synthesized Ag NPs containing polyacrylamide (PAm) hydrogel composites using free-radical cross-linking polymerization of acrylamide monomer in an  $\text{AgNO}_3$  aqueous medium. Wang, Li, Zhou, and Jia (2008) reported the preparation of magnetite nanoparticles induced by chitosan hydrogel under ambient conditions via iron (III): iron (II) ions assembly at different pHs.

K-carrageenan ( $\kappa\text{C}$ ) is a sulfated and linear polysaccharide with a repeating D-galactose and 3, 6-anhydro-D-galactose units (Nijenhuis, 1997; Zhai, Yi, Shu, Wei, & Ha, 1998) and is classically used as an agent for several potential pharmaceutical applications such as gelling agent in the food and pharmaceutical industries (Francis, Kumar, & Varshney, 2004) and controlled drug release

\* Corresponding author. Tel.: +60 7 5535577; fax: +60 7 5536163.

E-mail addresses: [idayu@cheme.utm.my](mailto:idayu@cheme.utm.my), [hhadi2@live.utm.my](mailto:hhadi2@live.utm.my) (I.I. Muhamad).

(Sipahigil & Dortunc, 2001; (Daniel-da-Silva et al., 2011; Nannaki, Karava, Kalantzi, & Bikiaris, 2010; Rasool, Yasin, Heng, & Akhter, 2010).

Different chemical modifications have been carried out to modulate physicochemical characteristics of carrageenan. Daniel-da-Silva et al. (2007) have modified carrageenans matrix to obtain suitable hydrogels for application in bone tissue engineering by coprecipitation of calcium phosphates into a  $\kappa$ -carrageenan matrix (Daniel-da-Silva et al., 2007). Gan and Feng (2006) synthesized carrageenan based composite hydrogels using nanohydroxyapatite and collagen for use as injectable bone substitute biomaterial for bone reconstruction surgery. Hosseinzadeh, Pourjavadi, Mahdavinia, and Zohuriaan-Mehr (2005) have prepared a very high absorptive  $\kappa$ -carrageenan hydrogel in saline with cross-linking of polyacrylamide and alkaline hydrolysis. The synthesized hydrogel exhibited the same water absorbance properties of  $\kappa$ -carrageenan copolymerized with acrylic acid (Pourjavadi, Harzandi, & Hosseinzadeh, 2004).

The aim of the present work is to fabricate new nanocomposite hydrogels by in situ approach to find a suitable drug carrier for GIT release. Ag and magnetite nanocomposite hydrogels are prepared and their performance in GIT conditions has been investigated. The effect of genipin cross-linking and nanoparticle loading on release performance is also studied and the most suitable nanocomposite is introduced.

## 2. Materials and methods

### 2.1. Materials

$\kappa$ -Carrageenan ( $\kappa$ C) (Sigma–Aldrich), Sodium carboxymethyl cellulose (NaCMC) (average molecular weight of 250,000, Acros Organic), methylene blue ( $C_{16}H_{18}ClN_3S \cdot 3H_2O$ ) (Riedel-de-Haën), ferric chloride hexahydrated ( $FeCl_3 \cdot 6H_2O$ ) (>99%, Sigma–Aldrich), ferrous chloride tetrahydrated ( $FeCl_2 \cdot 4H_2O$ ) (>99%, Sigma–Aldrich), ammonium hydroxide (28% ammonia in water) (99.99%, Fisher Chemicals), silver nitrate ( $AgNO_3$ ) (99.9%, AJAX Chemicals, Australia) and sodium borohydride ( $NaBH_4$ ) (Fluka). Distilled water was used in hydrogel synthesis and all chemicals are used as received with no further purification.

### 2.2. Preparation of $\kappa$ -carrageenan nanocomposites

#### 2.2.1. Preparation of modified $\kappa$ -carrageenan hydrogel

In order to increase the swelling ability of  $\kappa$ -carrageenan, it was blended with NaCMC in different concentrations. A typical hydrogels synthesis is as follows: 0.48 g of  $\kappa$ C was dissolved in 20 ml of distilled water at 80 °C and then mixed with a hot solution of 0.12 g NaCMC in 10 ml distilled water. The hot mixture was under gentle stirring for approximately 1 h to formulate a clear, viscous and homogenous solution with no bubbles. The system was under reflux to guarantee the water content of the system. Then, the resultant solution was poured into a ceramic mould to form the hardened hydrogel with a diameter of 3.5 cm and a thickness of 1.0 cm. Sample was allowed to equilibrate with ambient (25 °C) for 24 h to form the gel. Finally, hydrogel was dried at 37 °C in an oven overnight to form the desired hydrogel. Swelling properties of modified hydrogels were study immediately after drying process. For the sake of comparison, non-modified  $\kappa$ C hydrogels were also prepared using the same procedure.

#### 2.2.2. Preparation of Ag $\kappa$ -carrageenan nanocomposites

To synthesize the Ag NPs within the hydrogel matrix, the following steps were performed: The blank modified hydrogel was immersed in double distilled water to swell completely for 6.5 h (the time duration was found from swelling study of modified  $\kappa$ C)

to reach equilibrium. Then the fully swollen hydrogel was transferred to the silver nitrate solution with different concentrations for 4 h to obtain the silver ion loaded gels. Afterwards,  $Ag^+$  loaded samples were immersed in sodium borohydride ( $NaBH_4$ ) solution for almost 3 h to reduce the silver ions ( $Ag^+$ ) into silver particles ( $Ag^0$ ). The final Ag NPs were indicated by dark brown color formed in the hydrogel. The Ag hydrogel nanocomposites were washed with distilled water and then dried in an air oven at 40 °C over night.

#### 2.2.3. Preparation of magnetic $\kappa$ -carrageenan nanocomposites

In order to prepare magnetic nanocomposite hydrogels, in situ magnetic nanoparticles were carried out inside the hydrogel matrices by loading hydrogels with metal ions up to their maximum capacity. At first, the blank hydrogel was immersed in distilled water to swell up to its equilibrium for 6.5 h. The swollen hydrogel was placed in 100 ml of metal solution to absorb metal ions; then, it was kept in distilled water to remove unbound metal ions. Briefly, magnetic nanoparticles were prepared in two steps: First, swollen hydrogel was placed in Fe(II) and Fe(III) ion aqueous solution (Fe(II): Fe(III) ratio is 1:2) for 4 h to becomeloaded with metal ions. Second, the loaded hydrogel was soaked into distilled water to remove the unbound and/or physisorbed metal ions for another 2 h. After cleaning, iron ions (Fe(II) and Fe(III)) metal ion loaded hydrogels were transferred into 0.5 M sodium hydroxide solution to precede the reaction for 3 h. At the end, the hydrogels were cleaned by washing with distilled water and dried in an air oven at 40 °C over night. The synthesis conditions for all of the carrageenan nanocomposite carriers are listed in Table 1.

### 2.3. Measuring the swelling ratio

Both  $\kappa$ -carrageenan and  $\kappa$ -carrageenan/sodium carboxymethyl cellulose hydrogels ( $\kappa$ C/NaCMC) were immersed in different pH buffer solutions (pH 4, pH 6.5 and pH 8) at room temperature (25 °C) to investigate their swelling ability. Samples were placed in a Petri dish filled with 50 ml of the buffer solutions, separately. Filter paper was used to remove the surface water from swollen hydrogels prior to weighting. Then, swelling ratio (%) was determined using Eq. (1).

$$\text{Swelling ratio (\%)} = \left[ \frac{W_t - W_0}{W} \right] \times 100 \quad (1)$$

where  $W_t$  is the weight of swollen gels at predetermined time  $t$ , and  $W_0$  is the initial weight of samples. Samples were immersed in fresh buffer solution after weighting. Also, the test was carried out in triplicate and the calculated swelling ratios were reported in the mean values to maximize the accuracy.

### 2.4. Instrumentation

#### 2.4.1. FTIR analysis of hydrogel

3 mg of the dried samples (at 37 °C) of blank and loaded hydrogels were ground and then mixed with 10 times as much KBr powder. Hydraulic press was used to form the sample pellets under a pressure of 500 kg/cm<sup>2</sup>. Prepared samples were analyzed using a Fourier Transform Infrared Spectroscopy (FTIR) (Nicolet 670 FTIR,

**Table 1**  
Synthesis conditions of  $\kappa$ C hydrogels and nanocomposite hydrogels.

Sample Designation	$\kappa$ C (g)	NaCMC (g)	Nanofiller (gr/l)	Water (ml)
Blank $\kappa$ C	0.48	0.12	–	30
Ag-1.0	0.48	0.12	$AgNO_3$ 1.0%	30
Ag-1.5	0.48	0.12	$AgNO_3$ 1.5%	30
Ag-2.0	0.48	0.12	$AgNO_3$ 2.0%	30
M-1.0	0.48	0.12	Iron ions 1.0%	30
M-1.5	0.48	0.12	Iron ions 1.5%	30
M-2.0	0.48	0.12	Iron ions 2.0%	30

USA) with a 16 scan per sample in the region of 370–4000  $\text{cm}^{-1}$  with 1.0  $\text{cm}^{-1}$  interval and resolution of 4.

#### 2.4.2. UV/vis spectroscopy

1 ml of medium samples was poured in a container of Shelton UV/vis spectroscopy (ct 06484 USA) to determine the UV spectrum of the aliquots.

#### 2.4.3. Nanocomposites microstructure using field emission scanning electron microscope (FESEM/EDX)

Nanocomposites microstructure was studied using FESEM (Gemini Supra 35VP). Nanocomposites were mounted on a sample holder to be coated with gold using gold sputter coater Bio Rad Polaron Division (E6700, USA) under vacuum before observation. Sample photomicrographs was studied on FESEM at an accelerating voltage of 10 kV and different magnifications. Before FESEM measurements, samples were lyophilized. To keep the pores of the hydrogels intact for imaging, the nanocomposites were left in liquid nitrogen and then broken.

#### 2.5. In vitro MB release studies

To study the release profile of nanocomposites in a simulated gastrointestinal condition, methylene blue (MB) was used as a model drug due to its water solubility which facilitates an immediate visual inspection of the test. The loading process was during the preparation of the nanocomposites as described above. Samples were placed in Petri dishes filled with 60 ml of the medium solutions to study the release behavior. Petri dishes were placed in a thermostatic Kuhner Climo-Shaker (ISF1-X) at 37 °C and 120 rpm. The pH of the dissolution medium was kept at 0.1 N HCl for the first 10 min then changed to buffer solution pH 6.6 and finally pH 7.4 up to 30 min. At regular intervals of time, 1.0 ml aliquot of the medium solutions was removed from Petri dishes to determine its concentration. 1 ml of fresh buffer was replaced to maintain the original volume after withdrawal. All experiments were performed in triplicate. The withdrawn solution was diluted with KCl 1 M (dilution ratio 1:6) to make sure there is no interaction between the MB released and  $\kappa$ -carrageenan (Daniel-da-Silva, Ferreira, Gil, & Trindade, 2011; Soedjak, 1994).

The concentration of MB released was then measured using a UV/vis spectrophotometer at  $\lambda = 663 \text{ nm}$  which is the wavelength of maximum absorbance for MB according to Daniel-da-Silva et al. (2011). In their study, they reported that the addition of KCl to the aliquots prior to UV/vis analysis results in the disappearance of the absorbency of the complex at 559 nm and increased MB absorbance at 617 and 663 nm. Finally, the amount of cumulative release was determined from interpolation of standard calibration curve at 663 nm.

### 3. Results and discussion

#### 3.1. Characterization of modified $\kappa$ -carrageenan nanocomposites

The formation of silver nanocomposite structure in the blank hydrogel network can be expected since the silver salts loaded in blank hydrogel, reduced by  $\text{NaBH}_4$ , immediately turned into a dark brown color (Vimala, Samba Sivudu, Murali Mohan, Sreedhar, & Mohana Raju, 2009). For magnetic nanocomposite hydrogel, turning yellowish color of blank hydrogels into black color after 4 h indicate that the NPs were entrapped inside the carbohydrate polymers matrix (Ozay, Ekici, Baran, Aktas, & Sahiner, 2009).

FTIR spectra of the blank and nanocomposites hydrogels are shown in Fig. S1. Blank hydrogel showed a broad band in the range of 3411–3585  $\text{cm}^{-1}$ , attributed to the –NH asymmetric and –OH

symmetric stretching vibrations of the  $\kappa\text{C}/\text{NaCMC}$  hydrogel. The absorption bands at 2924  $\text{cm}^{-1}$  that appeared in all hydrogel spectrums is resulting from stretching frequency of –CH<sub>3</sub> groups. It can be seen that the asymmetric stretching band of –COOH occurs at the 1633  $\text{cm}^{-1}$  in the FTIR spectrum of  $\kappa\text{C}/\text{NaCMC}$  hydrogel. This peak has shifted to 1658 and 1653  $\text{cm}^{-1}$  in Ag and Magnetite nanocomposites.

Fig. S1 also shows that the characteristic absorptions of  $\kappa\text{C}/\text{NaCMC}$  hydrogel and Ag nanocomposite hydrogels are quite similar; however, the absorption bands in the range of 3411–3585  $\text{cm}^{-1}$ , changes and a peak at 3411  $\text{cm}^{-1}$  appears that this peak implies the interaction between the reduced Ag nanoparticles and COOH groups. A symmetrical stretching vibration of –COO<sup>–</sup> groups at 1420  $\text{cm}^{-1}$  is shifted to 1404  $\text{cm}^{-1}$  indicating the interaction of Ag nanofillers in the network. Also appeared peak at 2347  $\text{cm}^{-1}$  is intensified when Ag nanofillers are loaded.

For magnetic nanocomposite hydrogel, the absorption band at 1420  $\text{cm}^{-1}$  is also shifted to the lower wave number side of 1404  $\text{cm}^{-1}$  and the intensity of this peak is also increased with respect to nanocomposite formation. This peak displacement (–NH stretching and bending vibrations) is a result of the electrostatic interaction between the –NH and iron oxide nanoparticles (Sivudu & Rhee, 2009). –NH asymmetric and –OH symmetric stretching bands in magnetic nanocomposite spectrum have also shifted to lower regions at 3411 and 3204  $\text{cm}^{-1}$ , which indicates the interaction between the NPs and –COOH groups.

In order to verify the effect of the NPs on the microstructure of nanocomposites hydrogel, FESEM/EDX of the blank hydrogel and the NPs-loaded hydrogels (Ag-2.0 and M-2.0) are investigated (Fig. 1). The magnification of FESEM images was set at 2.5 K $\times$ . Clearly, loading NPs had changed the surface morphology of blank hydrogel. This shows the formation of NPs in the networks of blank hydrogel, whereas the blank hydrogel showed clear networks throughout the gel structure. Comparing magnetic nanofillers with Ag nanofillers, magnetic nanofillers formed more compact surface structure. Also, it is clear that nanofillers create a uniform structure when synthesized in the blank matrix which was more obvious in magnetic nanocomposites. Formation of NPs within the hydrogel network results in changing the porosity of hydrogels which can also affect the MB release from nanocomposite hydrogels. Energy dispersive X-ray (EDX) mode was also applied to investigate NPs distribution. It can be seen that the NPs have effectively uniform distribute throughout the hydrogel networks as shown in Fig. 1. The EDX spectrum also confirms the formation of metal NPs in the hydrogels. It is worthwhile to mention that Au element (FESEM coating element) was omitted from the EDX spectrum.

#### 3.2. Modification of $\kappa$ -carrageenan

As discussed above, blank hydrogel needs to be immersed in distilled water to reach its maximum swelling in order to be loaded with metal salts within its network. Since increasing the swelling ability of hydrogels can affect the ion loading in nanocomposites, sodium salt of carboxymethylcellulose (CMC) was chosen to be blended with  $\kappa\text{C}$  in order to increase its swelling ability in distilled water. NaCMC is the most widely used cellulose derivative (Kirk-Othmer, 2007, chap. 28). It is made by treating cellulose with sodium hydroxide and chloroacetic acid,  $\text{CH}_2\text{ClCOOH}$  in accordance to Williamson etherification reaction. Among all cellulose derivatives, only the sodium salt (NaCMC), is a polyelectrolyte, and thus a smart cellulose derivative which shows both pH sensitivity and ionic-strength variations. In addition, NaCMC has good swelling capability (Sannino, Demitri, & Madaghiele, 2009). The swelling rate of both modified and non-modified hydrogels in pH 6.5 is shown in Fig. S2, supplementary data. Clearly, 80:20 blend has the most swelling among all blend ratios and  $\kappa\text{C}$  non-blended



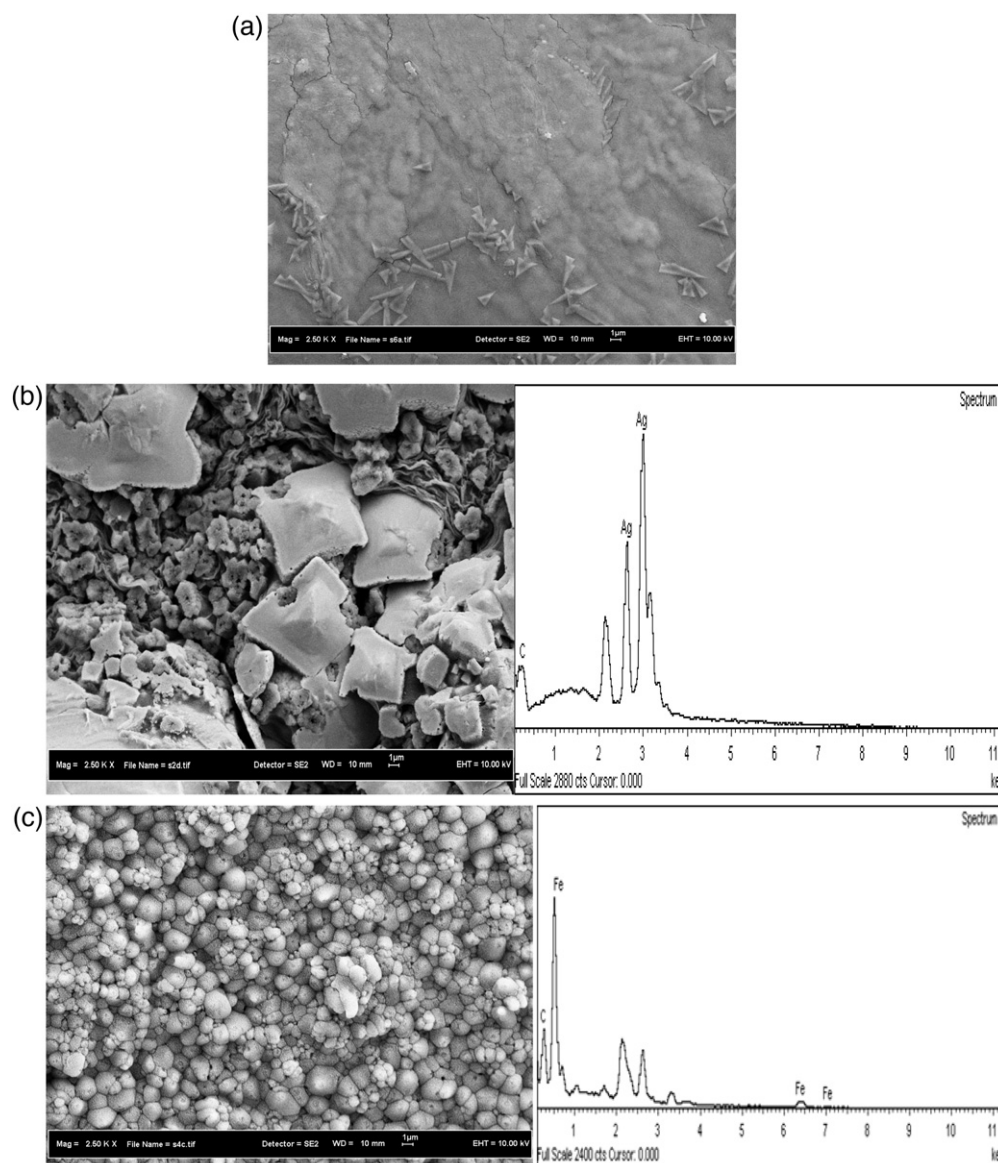


**Fig. 1.** FESEM microstructure and EDX spectrum of (a) blank hydrogel (b) Ag nanocomposites and (c) magnetite nanocomposite hydrogels.

hydrogel. An improvement in swelling capacity of modified hydrogels can be due to more hydrophilic chains or hydration of functional groups on the polymeric chains ( $-\text{OH}$ ) and ( $-\text{COOCH}_3\text{Na}$ ) (Berlin, Anderson, & Pallansch, 1973; Chen, Liu, & Tan, 2008). Increasing the  $\kappa\text{C}$  content of hydrogels results in a harder gel structure that hinders the swelling of hydrogel. On the other hand it was observed that in 70:30 and 60:40 blend ratios, hydrogels physical stability decreased and in the case of 60:40, erosion of hydrogel network stopped the swelling process. It was found that 80:20 ratio has both structure strength and network elasticity and can serve as an optimum ratio for the blend.

To study the behavior of modified  $\kappa\text{C}$  hydrogels in different pH, swelling tests were also carried out in buffer solution of pH 4 and 8. It was found that by increasing the medium pH, swelling ability of modified hydrogels increases, i.e., in pH acidic medium 80:20 blend ratio swelled the most and up to 9.52%; however, the swelling ratio in pH 6.5 and 8 was 16.63 and 19.61%, respectively. This behavior can be explained as follows: synthesized hydrogels are prepared in pH of distilled water ( $\text{pH } 6.25 \pm 0.25$ ), and since the  $\text{pK}_a$  of the carboxylic acid in the polysaccharide is almost 4.6,

ionization of the carboxylic acid groups occurs ( $\text{COO}^-$ ) (Taleb, El-Mohdy, & El-Rehim, 2009). Electrostatic repulsion force caused by the hydrogen bonds break down and this will lead to more water penetrating into the network. Therefore, the synergistic effect of negative-charges and hydrogen bonds justifies the water uptake behavior in the intermediate pH (Gorgieva & Kokol, 2011). At lower pH values, protonation of the carboxylic groups results in formation of more hydrogen bonds between the carboxylic acid groups in  $\kappa\text{C}$  hydroxyl groups. Therefore a more compact hydrogel structure with restricted movement and relaxation structure result in less swelling, reaching equilibrium swelling faster and less flexible network in acidic environment. On the other hand, in alkaline medium, ionization of carboxylic acid groups occurs in which these functional groups produce an electrostatic repulsion among polymer chains that expands the network allowing more water to penetrate the hydrogel network (Chen et al., 2009; Francis et al., 2004). In this experiment, 80:20 blend ratio exhibited the best swelling ability in all pH mediums, so this blend ratio was selected to be loaded with metal ions ( $\text{Ag}^+$ ,  $\text{Fe(II)}$  and  $\text{Fe(III)}$ ). In all cases in this article, 80:20 blend ratio is referred to as “blank hydrogel”.

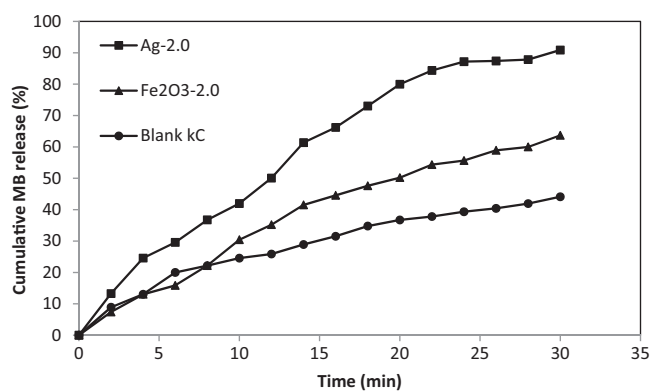


**Fig. 2.** In vitro MB release profile from the blank, Ag-2.0 and M-2.0 nanocomposites hydrogel under GIT conditions.

### 3.3. Effect of nanofillers on MB release in GIT stimuli

Fig. 2 shows the accumulative release profile of modeled drug in simulated gastrointestinal tract environment for all nanocomposite hydrogels. As shown in the Fig. 2, Ag nanocomposite hydrogel with 90.86% accumulated release showed the highest release compared to magnetite and blank hydrogels with 63.69 and 44.13% MB release, respectively, after 30 min. In stomach environment (pH 1.2), both magnetite and blank hydrogels showed almost the same release profile, and by changing the environment to Duodenum area, intestinal medium magnetite nanocomposite exhibited better performance and demonstrated more drug release in target environment (intestine) than blank hydrogel. The performance of each nanocomposite hydrogel is listed in Table 2. According to Table 2, although Ag-2.0 nanocomposite hydrogel has more release after 30 min, most of MB was released in stomach medium and only 10.89% was released in the intestine medium making it inefficient for gastro intestine drug delivery. On the other hand, magnetite nanocomposite released 30.43% of its MB loaded in stomach medium and 13.47% (almost 2 times more than Ag-2.0) MB was released in intestine. Briefly, although Ag-2.0 exhibited more MB release in all the release processes, its release was more pronounced in acidic medium (which is not desired) than intestinal medium (desired medium), but magnetite nanocomposite hydrogel exhibited better performance according to Table 2.

High cumulative release of Ag NPs loaded hydrogel can be attributed to the presence of Ag NPs colloids with high surface charges in the network. This results in a water afflux to balance the build-up of ion osmotic pressure (Wang, Flynn, & Langer, 2004). The distributed metallic nanoparticles can act as nanosized reservoirs for water from inside the polymer network. The vast interphase region between the nanoparticles and the network in the nanocomposite result in decreasing the characteristic diffusion length of water molecules through the nanocomposite hydrogels. These hydrophilic reservoirs then can quickly become

**Table 2**

The performance of blank, nanocomposite hydrogels and cross-linked nanocomposite hydrogels under GIT conditions.

	Stomach (pH 1.2) (%)	Duodenum (pH 6.6) (%)	Intestine (pH 7.4) (%)
Blank κC	24.56	12.17	7.39
Ag-2.0	71.30	13.02	10.89
M-2.0	30.43	19.78	13.47
Ag-2.0/GN0.5	37.17	21.08	30.43
Ag-2.0/GN1.5	27.17	23.26	36.08
M-2.0/GN0.5	26.52	8.26	6.30
M-2.0/GN1.5	20.65	16.52	14.34

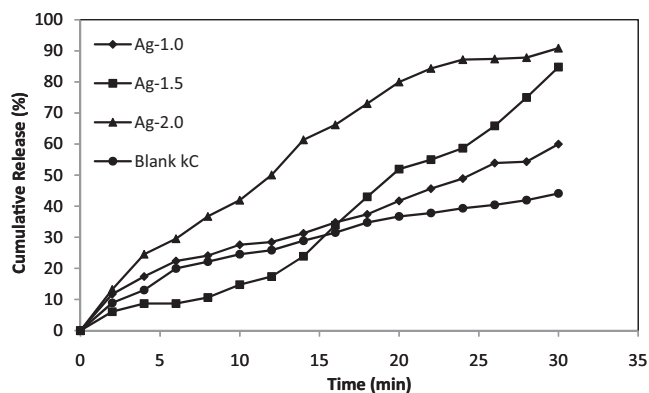


**Fig. 3.** The effect of Ag loading on MB release in GIT conditions.

dehydrated and act as water releasing channels for the interior water within the hydrogel network, the same as the hydrophilic PEO graft chains in comb-type hydrogels (Durme, Mele, Loos, & Du, 2005; Kaneko et al., 1998). During the experiment it was clear that the magnetic nanocomposite hydrogels were physically more stable (harder gels) than Ag nanocomposite hydrogels. FESEM images (See Fig. 1) also reveal that the surface morphology of magnetic hydrogel is more compact than that of Ag nanocomposites.

### 3.4. Effect of nanoparticles load on in vitro release profile

To improve the release properties of hydrogels, NPs loading was studied. Fig. 3 illustrates the in vitro release patterns of MB in simulated gastrointestinal tract environment vs. nanoparticles load for each nanocomposite hydrogels. Clearly, by increasing NPs concentration, nanocomposite hydrogels did not show the same release behavior in simulated medium.

In the case of Ag NPs loaded hydrogels, by increasing NPs release of MB is increased. Although the Ag-1.0 hydrogel did not show significant release changes in acidic and Duodenum mediums, when in contact with pH 7.4 (intestine environment), the Ag-1.0 cumulative release increased, indicating that more MB release in intestinal environment is achieved. An interesting phenomenon was observed in Ag-1.5 and Ag-2.0 nanocomposite hydrogels. Both hydrogels showed almost the same final cumulative MB release (84.76 and 90.86% for Ag-1.5 and Ag-2.0, respectively). But Ag-1.5 hydrogel behaved in a very different manner compared to Ag-2.0, that is, it showed exponential release profile. In stomach simulated environment, Ag-1.5 nanocomposite hydrogel has less MB release (14% compared to 71% in Ag-2.0) and by changing the medium to Duodenum area (pH 6.6) the MB release increases mildly and it accelerates in intestinal medium (pH 7.4) up to 84.76%. This behavior can be explained by NPs distribution in hydrogel matrix and reservoir role of NPs as discussed before. By increasing Ag NPs content in the hydrogel, agglomeration may occur which means that NPs create clusters that result in both increasing the NPs size and non-uniform distribution of particles. Uniform distribution of NPs acts as drug reservoirs inside the polymer matrix. Finer distribution of these nanoparticles within the matrix leads to more control over entrapped MB and smoother release. Consequently, these reservoirs will release the MB and act as drug releasing channels for the interior drugs. From the release profile, it can be concluded that the κC/NaCMC network is more suitable for formation of Ag-1.5 nanofillers than Ag-2.0. Fig. S3, supplementary data, the FESEM image of Ag-1.5 shows the less agglomeration and more uniform distribution of Ag NPs in the system.

Magnetic hydrogels displayed very different behaviors (Fig. 4). MB release in M-1.0 and M-1.5 hydrogels was less than blank hydrogel; however, M-2.0 showed more release (63.69% compared to

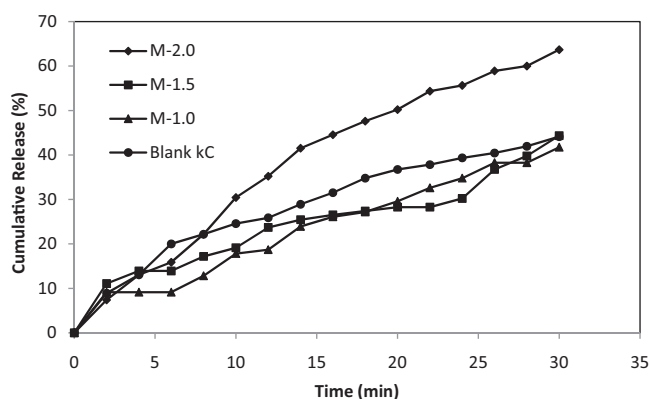


Fig. 4. The effect of magnetic ions loading on MB release in GIT conditions.

44.13% in blank hydrogel). As mentioned before, increasing the NPs content of hydrogels resulted in stronger hydrogels and this strength was obvious during the experiments. It is well known that swelling (and release) behavior of polyelectrolyte hydrogels is affected by the elastic properties of polymer matrix, ionic and mixing characteristics the surrounding media (Daniel-da-Silva et al., 2011; Goponenko & Asher, 2005; Peppas, Bures, Leobandung, & Ichikawa, 2000; Ricka & Tanaka, 1984). The elastic chemical potential difference is always against the swelling. Initially, the ionic chemical potential difference is great and controls the release in the system. When the equilibrium between internal and external ions is achieved, chemical potential difference controls the process. As the concentration of modified  $\kappa$ -carrageenan and the release media composition is kept constant, one possible explanation is the surface charge of magnetic NPs used as nanofillers (Daniel-da-Silva et al., 2011). Saravanan et al. (2007) indicated that the amount of charges entrapped within the hydrogel network, surface charge and the nanofillers concentration can affect the osmotic swelling in nanocomposites. According to Donnan's theory, it is expected that encapsulation of NPs within the hydrogel network results in a water afflux to balance the osmotic pressure buildup (Katchalsky, Lifson, & Eisenberg, 1951; Saravanan et al., 2007). This causes the hydrogel to expand its network more and consequently, more release will be observed. Here, M-1.0 and M-1.5 nanocomposite hydrogels cannot cause an afflux of water to balance the osmotic pressure buildup due to low NPs concentration. So the interaction of metal particles with the functional groups of hydrogels and also elastic chemical potential difference which is against the network expansion results in less MB release. However, by increasing the NPs content and in high concentration of magnetic NPs, in spite of stronger hydrogel network, the surface charge of magnetic NPs result in an afflux of water to balance the osmotic pressure buildup which causes the hydrogel to swell. This is in agreement with Daniel-da-Silva et al. (2011), Jiang et al. (2010) and Xiang and Chen (2007) findings and in contrast with the equilibrium swelling theory (Peppas et al., 2000) and some other former reports (Ozay et al., 2009; Paulino et al., 2011).

### 3.5. Effect of cross-linking on GIT release on nanocomposites

Ag-2.0 and M-2.0 nanocomposite hydrogels were cross-linked with genipin in two concentrations to study the effect of cross-linking on nanocomposite release. Genipin has been widely used in herbal medicine due to its anti-inflammatory, diuretic, choleretic and hemostatic properties. Recently, it has been used as a cross-linking agent in polymers (Meena, Prasad, & Siddhanta, 2009). This natural cross-linker is found to be 10,000 times less toxic compared to other cross linking agents (Muhamad, Fen, Hui, & Mustapha, 2011). To do the cross-linking, genipin in different concentrations

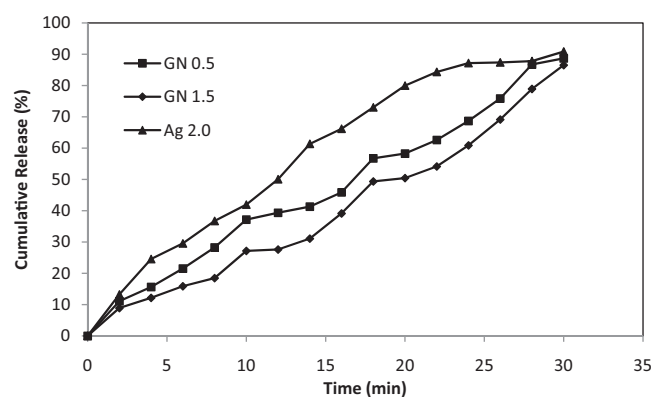


Fig. 5. MB release profile of cross-linked Ag nanocomposite hydrogels.

were added to the blank hydrogel. Then the cross-linked hydrogels were loaded with metal ions. As is clear from Fig. 5, by increasing the genipin content of nanocomposites, MB release in pH 1.2 and 6.6 decreases; however the release rate in pH 7.4 increases. This means that adding genipin to the nanocomposite has increased the efficiency of hydrogels (See Table 2). Ag-2.0/GN1.5 hydrogel released 36% of MB in intestinal medium, although only 10.89% of MB was released in Ag-2.0 hydrogel. The same results were observed for magnetite nanocomposite but the effect was less pronounced. M-2.0/GN1.5 nanocomposite, could release its MB loaded in intestine environment slightly more than blank hydrogels; however, it has still the advantage of less release in stomach environment (See Fig. 6 and Table 2).

Generally, cross-linking results in denser and more rigid hydrogel leading to a reduction in the degree of swelling in aqueous medium. As a result of these adjustments (as the amount of cross-linker increases, the pore size will decrease causing a decrease in swelling ratio), swelling characteristics can be regulated to a desired level. Also, increasing the cross-linker results in formation of smaller nanoparticles since the smaller free space for NPs formation is available. For each cross-linked nanocomposite hydrogel, the release in pH 1.2 medium was lower than the release in a pH 7.4 medium as a result of the formation of a hydrogen bond between the carboxymethyl cellulose due to the existence of carboxylic group ( $-\text{COOH}$ ) at low pH. By increasing the pH of medium, larger swelling force caused by the electrostatic repulsion between the ionized groups results in more MB release. As described in our previous work (Hezaveh, Muhamad, Fen, Ngadi, & Noshadi, in press), all the hydrogels have achieved higher swelling in buffer solution at pH 7.4 than that in acidic medium, pH 1.2 due to the change in ionic structure of the polymer when exposed to these medium.

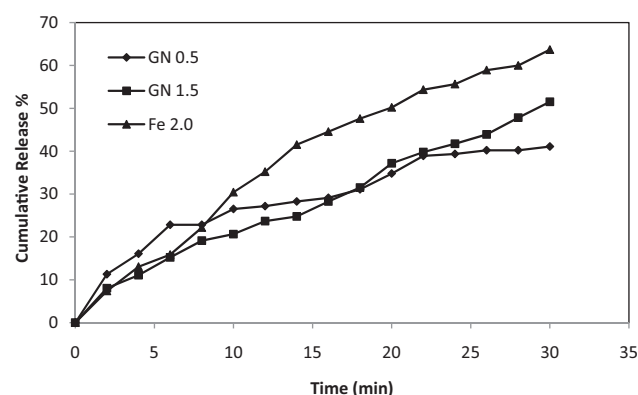


Fig. 6. MB release profile of cross-linked magnetite nanocomposite hydrogels.



#### 4. Conclusion

In this work, the effect of metallic NPs in gastrointestinal tract release of a modeled drug has been investigated. Two different nanocomposite hydrogels were synthesized and their performance in gastrointestinal condition was studied. It was found that incorporation of NPs can increase the MB release in GIT conditions. To improve the performance of nanocomposite hydrogels, the effect of NPs load and cross-linking (using genipin) was investigated. Ag-1.5 and Ag-2.0 nanocomposite hydrogels exhibited almost the same final cumulative MB release; however, Ag-1.5 showed less stomach release and more intestinal release making it more suitable than Ag-2.0. It is proposed that NPs can act as nano-sized reservoirs for water and the interphase region between the nanoparticles and the network can control the release properties. Better distribution and smaller NPs size can affect the release behavior.

It was found that low NPs concentration of magnetite nanocomposite hydrogels (M-1.0 and M-1.5) cannot cause a water afflux to balance the osmotic pressure buildup. So the interaction of metal particles with the functional groups of hydrogels and also elastic chemical potential difference which is against the network expansion results in less MB release. By increasing nanofiller loading in spite of a strong network, the surface charge of magnetic NPs result in an afflux of water to balance the osmotic pressure which causes more hydrogel swelling.

Cross-linking had a positive effect on release properties and showed that more targeted release will be achieved via genipin cross-linking. Both hydrogels exhibited better performance when cross-linked.

Comparing the performance of both nanocomposite hydrogels, it can be concluded that synthesizing Ag NPs in  $\kappa$ C/NaCMC hydrogels can improve the MB release in GIT conditions compared to magnetite. Also, monitoring the drug release in Ag nanocomposite hydrogels is more doable than magnetite nanocomposites.

#### Acknowledgments

We would like to thank the Food and Biomaterial Engineering lab, Bioprocess Engineering technicians and RUGrant vot 01H31 from Research Management Centre UTM for support of this study.

#### Appendix A. Supplementary data

Supplementary data associated with this article can be found, in the online version, at [doi:10.1016/j.carbpol.2012.02.062](https://doi.org/10.1016/j.carbpol.2012.02.062).

#### References

- Berlin, E., Anderson, B. A., & Pallansch, M. J. (1973). Water sorption by dried dairy products stabilized with carboxymethyl cellulose. *Journal of Dairy Science*, 56, 685–689.
- Cai, J., Guo, J., Ji, M., Yang, W., Wang, C., & Fu, S. (2007). Preparation and characterization of multiresponsive polymer composite microspheres with core-shell structure. *Colloid Polymer Science*, 285, 1607–1615.
- Chen, Y., Liu, Y., & Tan, H.-M. (2008). Preparation of macroporous cellulose-based superabsorbent polymer through the precipitation method. *Bioresources*, 3, 247–254.
- Chen, Y. H., Liu, Y. Y., Lin, R. H., & Yen, F. S. (2008). Characterization of magnetic poly(methyl methacrylate) microspheres prepared by the modified suspension polymerization. *Journal of Applied Polymer Science*, 108, 583–590.
- Chen, J., Liu, M., & Chen, Sh. (2009). Synthesis and characterization of thermo- and pH-sensitive kappa-carrageenan-g-poly(methacrylic acid)/poly(NN diethylacrylamide) semi-IPN hydrogel. *Materials Chemistry and Physics*, 115, 339–346.
- Chern, J. M., Lee, W. F., & Hsieh, M. Y. (2004). Preparation and swelling characterization of poly (n-isopropylacrylamide)-based porous hydrogels. *Journal of Applied Polymer Science*, 92, 3651–3658.
- Cho, K. H., Park, J. E., Osaka, T., & Park, S. G. (2005). The study of antimicrobial activity and preservative effects of nanosilver ingredient. *Electrochimica Acta*, 51, 956–960.
- Daniel-da-Silva, A. L., Trindade, T., Goodfellow, B. J., Costa, B. F. O., Correia, R. N., & Gil, A. M. (2007). In situ synthesis of magnetite nanoparticles in carrageenan gels. *Biomacromolecules*, 8, 2350–2357.
- Daniel-da-Silva, A. L., Moreira, J., Neto, R., Estrada, A. C., Gil, A. M., & Trindade, T. (2011). Impact of magnetic nanofillers in the swelling and release properties of carrageenan hydrogel nanocomposites. *Carbohydrate Polymers*, doi:10.1016/j.carbpol.2011.07.051
- Daniel-da-Silva, A. L., Ferreira, L., Gil, A. M., & Trindade, T. (2011). Synthesis and swelling behavior of temperature responsive kappa-carrageenan nanogels. *Journal of Colloid and Interface Science*, 355, 512–517.
- Durme, K. V., Mele, B. V., Loos, W., & Du, P. F. (2005). Introduction of silica into thermo-responsive poly(N-isopropyl acrylamide) hydrogels: A novel approach to improve response rates. *Polymer*, 46, 9851.
- Francis, S., Kumar, M., & Varshney, L. (2004). Radiation synthesis of superabsorbent poly(acrylic acid)-carrageenan hydrogels. *Radiation Physics and Chemistry*, 69, 481–486.
- Gan, S., & Feng, Q. (2006). Preparation and characterization of a new injectable bone substitute-carrageenan/nano-hydroxyapatite/collagen. *Zhongguo Yixue Kexueyuan Xuebao*, 28, 710–713.
- Goponenko, A. V., & Asher, S. (2005). Modeling of stimulated hydrogel volume changes in photonic crystal Pb2+ sensing materials. *Journal of the American Chemical Society*, 127, 10753–10759.
- Gorgieva, S., & Kokol, V. (2011). Synthesis and application of new temperature-responsive hydrogels based on carboxymethyl and hydroxyethylcellulose derivatives for the functional finishing of cotton knitwear. *Carbohydrate Polymers*, doi:10.1016/j.carbpol.2011.03.037
- Hezaveh, H., Fazlali, A., & Noshadi, I. (2012). Synthesis, rheological properties and magnetoviscous effect of Fe<sub>2</sub>O<sub>3</sub>/paraffin ferrofluids. *Journal of the Taiwan Institute of Chemical Engineers*, 43, 159–164.
- Hezaveh, H., Muhamad, I. I., Fen, L. S., Ngadi, N., & Noshadi, I. (in press) Swelling behaviour of cross-linked hydrogel based on blends of kappa-carrageenan and carboxymethyl cellulose: A controlled release study. *Journal of Microencapsulation*, doi:10.3109/02652048.2011.651501.
- Hosseinzadeh, H., Pourjavadi, A., Mahdavinia, G. R., & Zohuriaan-Mehr, M. J. (2005). Modified carrageenan 1: H-CarragPAM a novel biopolymer-based superabsorbent hydrogel. *Journal of Bioactive and Compatible Polymers*, 20, 475–490.
- Jiang, G. Q., Liu, C., Liu, X. L., Zhang, G. H., Yang, M., Chen, Q. R., et al. (2010). Swelling behavior of hydrophobic association hydrogels with high mechanical strength. *Journal of Macromolecular Science: Pure and Applied Chemistry*, 47, 663–670.
- Kakinoki, S., Taguchi, T., Saito, H., Tanaka, J., & Tateishi, T. (2007). Injectable in situ forming drug delivery system for cancer chemotherapy using a novel tissue adhesive: Characterization and in vitro evaluation. *European Journal of Pharmaceutical Biology*, 66, 383–390.
- Kaneko, Y., Nakamura, S., Sakai, K., Aoyagi, T., Kikuchi, A., Sakurai, Y., et al. (1998). Rapid deswelling response of poly(Nisopropylacrylamide) hydrogels by the formation of water release channels using poly(ethylene oxide) graft chains. *Macromolecules*, 31, 6099.
- Katchalsky, A., Lifson, S., & Eisenberg, H. (1951). Equation of swelling for polyelectrolyte gels. *Journal of Polymer Science*, 7, 57.
- Kirk-Othmer. (2007). *Food and feed technology* (5th Ed.). Wiley.
- Laurent, S., Forge, D., Port, M., Roch, A., Robic, C., Vander Elst, L., et al. (2008). Magnetic iron oxide nanoparticles: Synthesis, stabilization, vectorization, physicochemical characterizations, and biological applications. *Chemical Reviews*, 108, 2064–2110.
- Meena, R., Prasad, K., & Siddhanta, A. K. (2009). Development of a stable hydrogel network based on agar-kappa-carrageenan blend cross-linked with genipin. *Food Hydrocolloids*, 23, 497–509.
- Mi, F. L., Tan, Y. C., Liang, H. F., & Sung, H. W. (2002). In vivo biocompatibility and degradability of a novel injectable-chitosan-bead implant. *Biomaterials*, 23, 181–191.
- Muhamad, I. I., Fen, L. S., Hui, H. Ng., & Mustapha, N. A. (2011). Genipin-cross-linked kappa carrageenan/carboxymethyl cellulose beads and effects on beta-carotene release. *Carbohydrate Polymers*, 83, 1207–1212.
- Nagireddy, N. R., Yallapu, M. M., Kokkarachedu, V., Sakey, R., Kanikireddy, V., Alias, J. P., et al. (2011). Preparation and characterization of magnetic nanoparticles embedded in hydrogels for protein purification and metal extraction. *Journal of Polymer Research*, doi:10.1007/s10965-011-9642-2
- Nannaki, S., Karava, E., Kalantzi, L., & Bikiaris, D. (2010). Miscibility study of carrageenan blends and evaluation of their effectiveness as sustained release carriers. *Carbohydrate Polymers*, 79, 1157–1167.
- Nijenhuis, K. T. (1997). *Carrageenans. In Thermoreversible networks*. Berlin: Springer., pp. 203–252
- Ozay, O., Ekici, S., Baran, Y., Aktas, N., & Sahiner, N. (2009). Removal of toxic metal ions with magnetic hydrogels. *Water Research*, 43, 4403–4411.
- Paulino, A. T., Belfiore, L. A., Kubota, L. T., Muniz, E. C., Almeida, V. C., & Tambourgi, E. B. (2011). Effect of magnetite on the adsorption behavior of Pb(II), Cd(II), and Cu(II) in chitosan-based hydrogels. *Desalination*, 275, 187–196.
- Peppas, N. A., Bures, P., Leobandung, W., & Ichikawa, H. (2000). Hydrogels in pharmaceutical formulations. *European Journal of Pharmaceutics and Biopharmaceutics*, 50, 27–46.
- Pourjavadi, A., Harzandi, A. M., & Hosseinzadeh, H. (2004). Modified carrageenan 3: Synthesis of a novel polysaccharide-based superabsorbent hydrogel via graft copolymerization of acrylic acid onto kappa-carrageenan in air. *European Polymer Journal*, 40, 1363–1370.

- Rasool, N., Yasin, T., Heng, J. Y. Y., & Akhter, Z. (2010). Synthesis and characterization of novel pH-ionic strength and temperature-sensitive hydrogel for insulin delivery. *Polymer*, 51, 1687–1693.
- Reddy, K. R., Lee, K. P., Gopalan, A. I., & Kang, H. D. (2007). Organosilane modified magnetite nanoparticles/poly(aniline-co-o/m-aminobenzene sulfonic acid) composites: Synthesis and characterization. *Reactive and Functional Polymers*, 67, 943–954.
- Řicka, J., & Tanaka, T. (1984). Swelling of ionic gels: Quantitative performance of the Donnan theory. *Macromolecules*, 17, 2916–2921.
- Sannino, A., Demitri, C., & Madaghiele, M. (2009). Biodegradable cellulose-based hydrogels: Design and applications. *Materials*, 2, 353–373.
- Saravanan, P., Padmanabha Raju, M., & Alam, S. (2007). A study on synthesis and properties of Ag nanoparticles immobilized polyacrylamide hydrogel composites. *Materials Chemistry and Physics*, 103, 278–282.
- Sipahigil, O., & Dortunc, B. (2001). Preparation and in vitro evaluation of verapamil HCl and ibuprofen containing carrageenan beads. *International Journal of Pharmaceutics*, 228, 119–128.
- Soedjak, H. S. (1994). Colorimetric determination of carrageenans and other anionic hydrocolloids with methylene blue. *Analytical Chemistry*, 66, 4514–4518.
- Souza, G.I.H., Marcato, P.D., Durañ, N.E. (2004). *Esposito, Utilization of Fusarium oxysporum in the biosynthesis of silver nanoparticles and its antibacterial activities*, Presented at Xth National Meeting of Environmental Microbiology, Curitiba, PR (Brazil) [Abstract pp. 25].
- Taleb, M. F. A., El-Mohdy, H. L. A., & El-Rehim, H. A. A. (2009). Radiation preparation of PVA/CMC copolymers and their application in removal of dyes. *Journal of Hazardous Materials*, 168(1), 68–75.
- Tan, M. L., Choong, P. F. M., & Dass, C. R. (2010). Recent developments in liposomes microparticles and nanoparticles for protein and peptide drug delivery. *Peptides*, 31, 184–193.
- Vimala, K., Samba Sivudu, K., Murali Mohan, Y., Sreedhar, B., & Mohana Raju, K. (2009). Controlled silver nanoparticles synthesis in semi-hydrogel networks of poly(acrylamide) and carbohydrates: A rational methodology for antibacterial application. *Carbohydrate Polymers*, 75, 463–547.
- Wang, C., Flynn, N. T., & Langer, R. (2004). Controlled structure and properties of thermoresponsive nanoparticle-hydrogel composites. *Advanced Materials*, 16(13), 107.
- Wang, Y., Li, B., Zhou, Y., & Jia, D. (2008). Chitosan-induced synthesis of magnetite nanoparticles via iron ions assembly. *Polymers for Advanced Technologies*, 191, 256–1261.
- Xiang, Y., & Chen, D. (2007). Preparation of a novel pH-responsive silver nanoparticle/poly (HEMA-PEGMA-MAA) composite hydrogel. *European Polymer Journal*, 43, 4178–4187.
- Zhai, M. L., Yi, M., Shu, J., Wei, J. S., & Ha, H. F. (1998). Radiation preparation and diffusion behavior of thermally reversible hydrogels. *Radiation Physics and Chemistry*, 52, 313–316.